American Mineralogist, Volume 88, pages 676–685, 2003

Contribution to the mineralogy of acid drainage of Uranium minerals: Marecottite and the zippeite-group

J. BRUGGER,[1,2,*] PETER C. BURNS,[3] AND N. MEISSER[4]

[1]Department of Geology and Geophysics, The University of Adelaide, North Terrace, 5005 Adelaide, South Australia
[2]Division of Mineralogy, South Australian Museum, North Terrace, 5000 Adelaide, South Australia
[3]Department of Civil Engineering and Geological Sciences, 156 Fitzpatrick Hall, University of Notre Dame, Notre Dame, Indiana 46556-0767, U.S.A.
[4]Musée Géologique Cantonal & Laboratoire des Rayons-X, Institut de Minéralogie, UNIL-BFSH2, CH-1015 Lausanne-Dorigny, Switzerland

ABSTRACT

Sulfate-rich acid waters produced by oxidation of sulfide minerals enhance U mobility around U ores and U-bearing radioactive waste. Upon evaporation, several secondary uranyl minerals, including many uranyl sulfates, precipitate from these waters. The zippeite-group of minerals is one of the most common and diverse in such settings. To decipher the nature and crystal chemistry of the zippeite-group, the crystal structure of a new natural hydrated Mg uranyl sulfate related to Mg-zippeite was determined. The mineral is named marecottite after the type locality, the La Creusaz U prospect near Les Marécottes, Western Swiss Alps.

Marecottite is triclinic, $P\bar{1}$, with a = 10.815(4), b = 11.249(4), c = 13.851(6) Å, α = 66.224(7), β = 72.412(7), and γ = 69.95(2)°. The ideal structural formula is $Mg_3(H_2O)_{18}[(UO_2)_4O_3(OH)(SO_4)_2]_2(H_2O)_{10}$. The crystal structure of marecottite contains uranyl sulfate sheets composed of chains of edge-sharing uranyl pentagonal bipyramids that are linked by vertex-sharing with sulfate tetrahedra. The uranyl sulfate sheets are topologically identical to those in zippeite, $K(UO_2)_2(SO_4)O_2 \cdot 2H_2O$. The zippeite-type sheets alternate with layers containing isolated $Mg(H_2O)_6$ octahedra and uncoordinated H_2O groups. The uranyl sulfate and Mg layers are linked by hydrogen bonding only.

Magnesium-zippeite is redefined as $Mg(H_2O)_{3.5}(UO_2)_2(SO_4)O_2$, based on comparison of the powder X-ray diffraction pattern of micro-crystalline co-type material with the pattern of a synthetic phase. Magnesium-zippeite contains zippeite-type uranyl sulfate sheets with Mg located between the layers, where it is in octahedral coordination. In Mg-zippeite, distorted Mg octahedra are linked by sharing vertices, resulting in dimers. The apices of the Mg octahedra correspond to two O atoms of uranyl ions, and four H_2O groups.

Magnesium-zippeite and marecottite co-exist, sometimes in the same sample, at Lucky Strike no. 2 mine, Emery County, Utah (type locality of Mg-zippeite), at Jáchymov, Czech Republic, and at La Creusaz. This study provides insight into the complexity of the zippeite-group minerals containing divalent cations, where different arrangements in the interlayers result in different unit cells and space groups.

INTRODUCTION

U sulfates and acid leaching of U minerals

The oxidation of sulfides by oxygen-bearing waters produces sulfate-rich (>1000 ppm SO_4^{2-}) acid (pH < 5) waters that can leach and transport large quantities of heavy metals (e.g., Edwards et al. 2000; Evangelou and Zhang 1995). Such waters are responsible for large-scale mobility of U and other actinides around U-bearing mine sites and tailing dumps, even long after mining has ceased (e.g., Fernandes et al. 1995). Acid sulfate waters also may be present in and around high-level radioactive waste deposits, in particular those located in sulfide-bearing host-rocks such as shales (e.g., the proposed Swiss repository in Mesozoic shales; Thury and Bossart 1999; Vinard et al. 1993). Available thermodynamic data (Cox et al. 1989; Grenthe et al. 1992; Shock et al. 1997) indicate that U^{6+} sulfate complexes, mainly $UO_2(SO_4)_{aq}$, are the principal aqueous species responsible for the high U solubility under those conditions (Fig. 1). In contrast, U^{6+} carbonate complexes become dominant under neutral and alkaline conditions (Fig. 1).

Uranium sulfate minerals commonly are widespread around U-bearing mine sites, where they usually form during the evaporation of acid sulfate-rich mine drainage waters (Finch and Murakami 1999). Uranopilite, $(UO_2)_6(SO_4)(OH)_{10} \cdot 12H_2O$ (Burns 2001); johannite, $Cu(UO_2)_2(SO_4)_2(OH)_2 \cdot 8H_2O$ (Cejka et al. 1988); schröckingerite, $NaCa_3(UO_2)(SO_4)(CO_3)_3F \cdot 10H_2O$; coconinoite $Fe_2Al_2(UO_2)_2(PO_4)_4(SO_4)(OH)_2 \cdot 20H_2O$; and zippeite-group minerals are the most common uranyl sulfates. In addition, several new uranyl sulfates have been described recently: deliensite, $Fe(UO_2)_2(SO_4)_2(OH)_2 \cdot 3H_2O$ (Vochten et al. 1997); jáchymovite, $(UO_2)_8(SO_4)(OH)_{14} \cdot 13H_2O$ (Cejka et al. 1996); and rabejacite, $Ca(UO_2)_4(SO_4)_2(OH)_6 \cdot 6H_2O$ (Deliens and Piret 1993). The latter phases may be more widespread than

* E-mail: Brugger.Joel@saugov.sa.gov.au

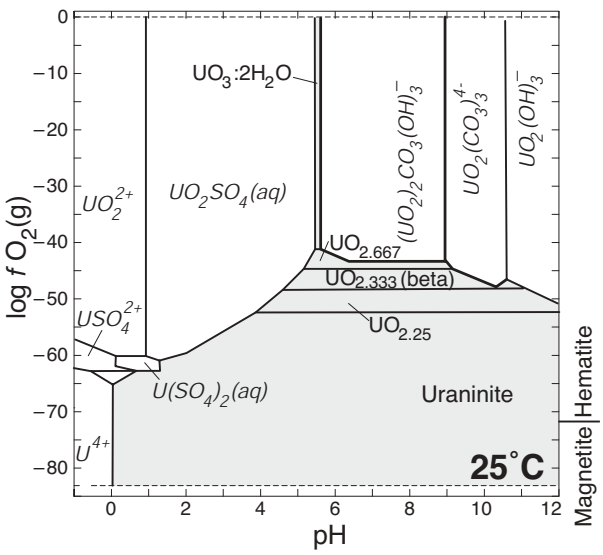

FIGURE 1. Fugacity of oxygen vs. pH diagram for U in sulfate- and carbonate-bearing waters, showing that uranyl carbonate complexes dominate in slightly acid to basic waters, whereas uranyl sulfate complexes dominate in strongly acid waters. Aqueous species are labeled in italics, and minerals in straight text. Thermodynamic data from Cox et al. (1989), Grenthe et al. (1992), and Shock et al. (1997). T = 25 °C, activity of U species 10^{-5} m, activity of carbonate species 10^{-3} m, and of sulfate species 10^{-2} m.

originally thought; since its description in 1993, rabejacite has been recognized from several localities (e.g., La Creusaz, Swiss Alps and Jáchymov, the Krusne hory Mts., Czech Republic; Sejkora et al. 2000), locally in large quantities (e.g., Ranger mine, Northern Territories, Australia; Dermot and Brugger 2000).

The example of rabejacite illustrates some of the difficulties in characterizing uranyl sulfate assemblages. Indeed, little is known about the crystal chemistry of the uranyl sulfates, despite the importance of these phases in controlling the concentration of U in mine-drainage waters, and the distribution of U around such sites. Because these minerals typically occur as microcrystalline crusts, commonly finely intergrown with other U sulfates and/or mono-carbonates, crystal-chemical studies are difficult. The crystal structures of natural schröckingerite (Mereiter 1986), johannite (Mereiter 1982), and recently uranopilite (Burns 2001) have been solved, but the nature (unit cell and chemical formula) of some widespread phases, like the zippeite-group minerals, remains speculative. In their recent review of the mineralogy and paragenesis of U minerals, Finch and Murakami (1999) state that "re-examination of the zippeite-group is in order, a potentially daunting challenge given the extremely small grain size and pulverulent habits common to most zippeite-group minerals (p. 136)."

We present the results of the first crystal structure determination for a natural mineral related to Mg-zippeite that formed during acid mine drainage at the La Creusaz Prospect, Swiss Alps. In light of these data, we review the available chemical and structural information pertaining to the zippeite group. Magnesium-zippeite is redefined, and the new Mg uranyl sulfate marecottite is defined as a member of the zippeite-group.

MINERALOGY OF THE ZIPPEITE-GROUP

Details of the chemistry of the zippeite group have been controversial since the naming of the first member of the group by Haidinger (1845). The importance of cations such as K, Na, Mg, Ni, and Co as fundamental constituents of this mineral group was recognized by Frondel et al. (1976). On the basis of natural assemblages and synthesis products, Frondel et al. (1976) distinguished two families of zippeites, those containing monovalent cations, and those containing divalent cations. No solid solution was observed between the two families, but extensive solid solutions were recognized within the zippeites with divalent cations. Frondel et al. (1976) proposed the following general chemical formula for zippeite: $A_x(UO_2)_6(SO_4)_3(OH)_{10}.yH_2O$, with A = K^+, Na^+, NH_4^+ (x = 4, y = 4), or A = Ca^{2+}, Ni^{2+}, Fe^{2+}, Mn^{2+}, Mg^{2+}, Zn^{2+} (x = 2, y = 16).

The latest classification of U minerals is based on the polymerization of those polyhedra of higher bond-valence (Burns 1999). The zippeite-type sheet involves chains of edge-sharing uranyl pentagonal bipyramids two polyhedra wide, which are linked by sharing vertices with sulfate tetrahedra. This sheet occurs in synthetic zippeite (Vochten et al. 1995; see below). No structure analysis is available for natural zippeite.

MARECOTTITE, A NEW MINERAL

La Creusaz U prospect

The La Creusaz U prospect near Les Marécottes village (canton Valais, Western Alps, Switzerland) was discovered in 1973, and is one of the major finds resulting from frantic prospecting for U in the 1960s and 1970s, aimed at evaluating Swiss strategic reserves (Gillieron 1988; Stüssi-Lauterburg 1995). The prospect was explored using drill holes, surface scratching (shallow trenches of ~1 m), and tunnels between 1973 and 1981. The mineralization occurs in hydrothermal breccia veins at the contact between the pre-Variscan gneissic basement of the Aiguilles Rouges Massif and the Carboniferous Vallorcine granite (Meisser and Ansermet 1996; Meisser et al. 2002). The primary mineralization event, probably Permo-Carboniferous in age (Meisser et al. 2002), resulted in the precipitation of uraninite and pyrite. It was followed by a second mineralization stage characterized by intense brecciation and silicification, with precipitation of minor amounts of siderite, chalcopyrite, sphalerite, Se-bearing galena, and laitakarite, $Bi_4(Se, S)_3$. Several episodes of remobilization have produced complex mineral assemblages and textures at La Creusaz. The opening of the Tethys Ocean during the Late Triassic resulted in fracturing and intense fluid circulation, which probably led to the formation of rare seleniosels [wittite, $Pb_3Bi_4(S, Se)_9$ and weibullite, $Pb_5Bi_8(Se, S)_{18}$] by sulfidation of laitakarite ± Se-rich galena (Meisser and Beck 2000). During the Tertiary metamorphism under lowest greenschist-facies conditions, the ores were partially remobilized, and abundant clinochlore together with minor bursaite, coffinite, arsenopyrite, and Se-poor galena crystallized in veins.

^{230}Th-^{234}U disequilibrium dating of uranophane-α gives an

age of 138 000 ± 10 000 years, showing that the major supergene alteration of the La Creusaz deposit is coeval with the beginning of the interglacial Riss-Wurm period (Meisser and Ansermet 1996; Meisser et al. 2002). At that time, the melting of the ice sheet produced rapid decompression, uplift, and fracturing of the rocks, followed by intense fluid circulation. This series of events resulted in the formation of a complex assemblage of uranyl-bearing minerals at La Creusaz, characterized mainly by the coexistence of silicates, oxy-hydroxides, arsenates, and phosphates.

Since the end of the underground exploration in 1981, exposed veins and stockpiled U ore have been subjected to acid mine drainage water and atmospheric oxygen in the abandoned galleries. Oxidation of the sulfides (mainly pyrite and chalcopyrite) in the presence of strong bacterial activity resulted in the production of acid (pH ≥ 3.1), sulfate-rich waters. These waters reacted with uraninite, clinochlore, illite, calcite, and siderite to form a rich assemblage of secondary uranyl minerals, including several U sulfates. The mining activity and the subsequent water circulation resulted in a halo of contamination by U, ^{206}Pb (decay product of ^{238}U), and other heavy metals around the site (Pfeifer et al. 1994).

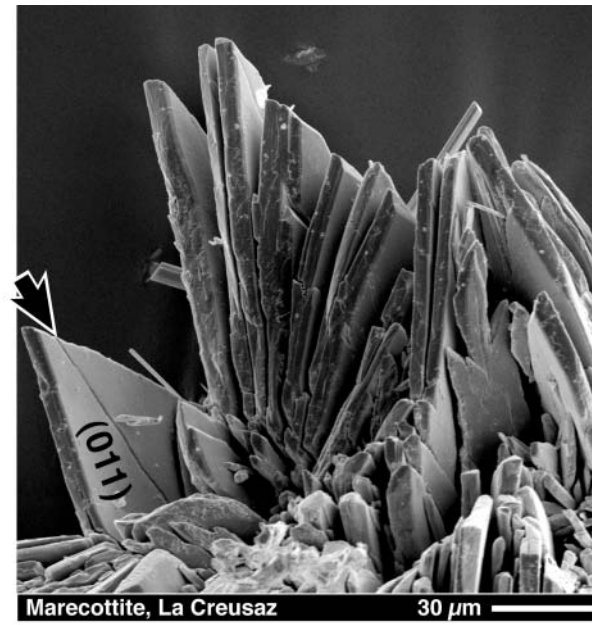

FIGURE 2. SEM image of a typical marecottite aggregate from La Creusaz, Swiss Alps. Note the perfect cleavage along (011) and the trace of the twin composition plane (arrow).

Occurrence and physical properties

The marecottite holotype sample (MGL58285) is a small (3 × 2 cm) uraninite (with minor chalcopyrite) fragment collected from among the ore stockpiled in the exploration tunnel at La Creusaz, and undisturbed since 1981. The uraninite is covered by gypsum and tiny orange crystals of marecottite. On other larger samples, and especially in the cotype, marecottite is directly associated with rabejacite, johannite, a new cryptocrystalline light-green hydrated U-Cu-sulfate (IMA 2000-019), an earthy pale-yellow U-sulfate-phosphate related to coconinoite, ktenasite, and jarosite. Other neoformed secondary uranyl-bearing minerals observed in the sampled area are zippeite sensu stricto, Mg-zippeite, jáchymovite, zeunerite, two new finely crystallized yellow U-Ca-sulfates, and a new earthy yellow U-sulfate.

Marecottite has been accepted as a new mineral by the Commission on New Minerals and Mineral Names of the International Mineralogical Association (vote IMA2001-056), and the type material is deposited at the Musée Géologique Cantonal of Lausanne, Switzerland (holotype MGL58285 and cotype MGL58290). The name refers to the village of Les Marécottes, whose church is only 1100 m from the type locality.

Marecottite occurs as diamond-shaped platelets flattened along (011) that reach 500 μm in length (Fig. 2). Hence, the pinacoid {011} is the prominent form. The crystals commonly consist of two twinned individuals, with composition plane corresponding to the long axis of the crystal and perpendicular to {011}. The crystals are grouped into rosettes. The Mohs' hardness is ~3, but the mineral is very brittle and displays a perfect cleavage along (011). Marecottite sinks in Clerici solution (ρ = 4.03), but the density calculated from the crystal structure is 3.83 g/cm^3. This discrepancy may be due to cationic exchange of Mg for Tl. Marecottite is transparent, yellow-orange, with colorless streak and vitreous luster. No UV fluorescence has been observed under short or long wavelengths. The mineral is optically biaxial. The range of refractive indices measured in the (011) face is n = 1.735–1.750. The mineral displays a fair pleochroism in the (011) face, from pale-yellow to orange-yellow.

Chemical composition

Electron microprobe (EMP) analyses were performed on a CAMECA SX-50 instrument operated in WDS mode at 15 kV and 25 nA, with a 5 μm diameter beam. Pure metallic U and metallic Mn, synthetic MgO, and natural barite were used as standards. The size of the beam was limited by the size of the crystals mounted in epoxy resin, and was not sufficient to avoid significant sample damage during the analysis. This problem, together with a poor sample polish, resulted in greatly varying analytical sums (68 to 91 wt%). Analysis of other uranyl sulfates (natural rabejacite, uranopilite, and zippeite; synthetic $UO_2SO_4 \cdot 0.5H_2O$) shows that, despite large variations in analytical totals, the average analyses are close to the values expected from the chemical formulae for these phases. The S values, however, were systematically low, and a correction factor of 1.222 was applied off-line, which brought the U/S atomic ratio for all the mentioned phases within 5% of the expected values for the know phases. These low S values may be due to problems with the PAP correction procedure for S in the presence of large amounts of U. This problem could be avoided by using a matrix-matched S-standard, but none of the investigated U-sulfate was suitable for use as standard, mainly due to the poor polish.

The semi-quantitative chemical analyses (Table 1) show that the U/S ratio in marecottite is close to 2 (2.08). Among the divalent cations, Mg is the most abundant and Mn is the second-most abundant, with an Mg/Mn ratio of about 3.5. Other

TABLE 1. Comparison of the chemical and crystallographic data on zippeite, Mg-zippeite, and marecottite

	Zippeite			Mg-zippeite "original"		Mg-zippeite "redefined"	Marecottite	
Reference	Frondel et al. (1976)		Vochten et al. (1995)	Frondel et al. (1976)		Spitsyn et al. (1982) and this study	This study	
Formula	$K_4(UO_2)_6(SO_4)_3(OH)_{10}.4H_2O$		$K(UO_2)_2(SO_4)O_2•2H_2O$ (?) (mod. this study)	$Mg_2(UO_2)_6(SO_4)_3(OH)_{10}.16H_2O$		$Mg(H_2O)_{3.5}(UO_2)_2(SO_4)O_2$	$Mg_3(H_2O)_{18}[(UO_2)_4O_3(OH)(SO_4)_2]_2(H_2O)_{10}$	
Material source	Synthetic compound		Synthetic compound	Natural, Lucky Strike N.2 mine, Utah, USA		Synthetic(structure on Zn-isomorph)	Natural, La Creusaz, Western Swiss Alps	
Chemistry	Meas	Calc	Calc	Meas	Calc	Calc	Meas†	Calc
K_2O	7.89	8.17	6.32					
MgO	n.d.		n.d.	MgO 6.2 CoO 1.4	3.72	5.34	MgO 2.03 MnO 1.15	3.33
UO_3	75.38	74.39	76.86	74.6	70.37	75.72	66.36	71.05
SO_3	11.41	10.41	10.86	5.0	9.84	10.60	8.95	9.94
H_2O	4.92	7.03	6.06	10.9	16.07	8.35	14.73 (calc)	15.66
Total	99.60	100	100	98.1	100	100	93.2	100
Unit cell	*		*C*2/c	*		*C*2/m	*P*$\bar{1}$	
a			8.755			8.654(3)	10.815(4)	
b			13.987			14.182(6)	11.249(4)	
c			17.73			17.714(7)	13.851(6)	
α							66.224(7)	
β			104.13			103.92	72.412(7)	
γ							69.95(2)	

* No cell is given by Frondel et al. (1976) for any zippeite containing a divalent cation instead of a monovalent cation.
† Semi-quantitative electron microprobe analysis, average of 8 points.

possible cations such as Ca, Al, Fe, Cu, Sr, Pb, K, and Na have been measured, but appear to be below the detection limit of about 0.05 wt% oxide.

The FT-IR spectrum of marecottite, collected using a diamond cell GRAESEBY SPECAC/PARAGON 1000 on ground material for wavenumbers between 600 and 4000 cm^{-1}, shows a broad asymmetric stretching mode of H_2O (υ H_2O) at 3343 cm^{-1} and a band of similar intensity corresponding to the bending vibration (δ H_2O) at 1613 cm^{-1}. The width of the υ H_2O band (3575 cm^{-1} to ~2000 cm^{-1}) indicates a complex network of hydrogen bonding in this mineral. The υ_3 UO_2^{2+} band at 895 cm^{-1} is similar to the υ_3 UO_2^{2+} band in synthetic zippeite-group minerals (873–924 cm^{-1}; Cejka 1999). The marecottite FT-IR spectrum also displays several bands attributed to vibrations within the SO_4^{2-} groups: υ_4 SO_4^{2-} at 630 cm^{-1} and two bands attributed to the triply degenerate υ_3 SO_4^{2-} mode at 1085 and 1138 cm^{-1}. The location of these bands is very similar to that in synthetic zippeites and in natural johannite (Cejka 1999).

SINGLE CRYSTAL STUDY AND CRYSTAL STRUCTURE OF MARECOTTITE

X-ray data

A single crystal with approximate dimensions $80 \times 80 \times 15$ μm^3 was selected that exhibited uniform optical properties and sharp extinction between crossed polarizers. It was mounted on a Bruker Platform 3-circle goniometer equipped with a 1K SMART CCD (charge-coupled device) detector. The data were collected using monochromatic Mo$K\alpha$ X-radiation and frame widths of 0.3° in ω. Unit-cell dimensions (Table 2) were refined on the basis of 214 reflections using least-squares techniques. A sphere of three-dimensional data was collected for $3° \le 2\theta \le 56.7°$; intensities were integrated and corrected for Lorentz polarization and background effects using the Bruker program SAINT. An empirical absorption correction was done on the basis of the intensities of equivalent reflections, and it reduced R_{int} of 309 intense reflections from 7.7 to 5.3%. A total of 8992 reflections were collected, and merging of equivalent reflections gave 6526 unique reflections (R_{int} = 11.1%) with 2473 classed as observed ($|F_o| \ge 4\sigma_F$).

TABLE 2. Miscellaneous information pertaining to the structure determination of marecottite

a (Å)	10.815(4)	Crystal size (μm)	80×80×15 μm³
b (Å)	11.249(4)	μ (mm^{-1})	23.2
c (Å)	13.851(6)	D_{calc} (g/cm^3)	3.827
α (°)	66.224(7)	Total ref.	8992
β (°)	72.412(7)	Unique ref.	6526
γ (°)	69.955(11)	R_{int} (%)	11.1
V (Å³)	1422.1(9)	Unique $\|F_o\| \ge 4\sigma_F$	2473
Space group	*P*$\bar{1}$	Final *R*1* (%)	7.9
F(000)	1448.6	*S*†	0.82

Unit-cell contents: $(Mg_{2.18}Mn_{0.82})(H_2O)_{18}[(UO_2)_4O_3(OH)(SO_4)_2]_2(H_2O)_{10}$

* $R1 = \Sigma(|F_o| - |F_c|)/\Sigma|F_o|$.
† $S = [\Sigma w(|F_o| - |F_c|)^2/(m - n)]^*$, for *m* observations and *n* parameters.

Structure solution and refinement

Scattering curves for neutral atoms, together with anomalous dispersion corrections, were taken from Ibers and Hamilton (1974). The Bruker SHELXTL Version 5 system of programs was used for the refinement of the crystal structure.

Reflection statistics indicated space group *P*$\bar{1}$, which was verified by the successful solution of the structure by direct methods. The structure was refined on the basis of F^2 for all unique data. The final model included all atomic positional parameters, anisotopic displacement parameters for the cations, isotropic displacement parameters for the anions, and a weighting scheme of the structure factors. The occupancies of the three *M* sites (*M* = divalent metal cation) were refined using the scattering factors of Mg and Mn, with the occupancy of each site constrained to unity. The final agreement index (*R*1) of 7.9% was calculated using the 2473 observed reflections. A model including anisotropic displacement of the anions was tried, but some of the displacement parameters became unrealistic. In the final cycle of refinement, the average parameter shift/ESD was less than 0.0005. The minimum and maximum peaks in the final difference-Fourier maps were 5.08 and –4.37 e/Å³, and were located within 1 Å of the U atoms. The atomic-posi-

tional parameters and anisotropic-displacement parameters are given in Tables 3 and 4, and selected interatomic distances and angles are given in Table 5. Calculated and observed structure factors are provided in Table 6[1]. The calculated and measured powder X-ray diffraction (XRD) patterns are compared in Table 7.

RESULTS OF THE STRUCTURE DETERMINATION

Cation polyhedra

The structure contains four symmetrically unique U^{6+} cations, each of which is strongly bonded to two O atoms, forming approximately linear $(UO_2)^{2+}$ uranyl ions (designated *Ur*), with U-O_{Ur} bond lengths of ~1.8 Å. Each uranyl ion is coordinated by five anions that are located at the equatorial vertices of pentagonal bipyramids, with the O_{Ur} atoms located at the apices of the bipyramids. The average U-ϕ_{eq} (ϕ = O, OH^-; eq = equatorial) bond-lengths for each polyhedron range from 2.38 to 2.40 Å, in good agreement with the average distance of

[1]For a copy of Table 6, Document AM-03-029 contact the Business Office of the Mineralogical Society of America (see inside front cover of recent issue) for price information. Deposit items may also be available on the American Mineralogist web site (see inside back cover of a current issue for a web address).

TABLE 3. Atomic position parameters (×10^4), equivalent isotropic-displacement parameters (Å^2 ×10^3) and bond valence calculations (BVC) for the structure of marecottite.

	x	*y*	*z*	*U_{eq}	BVC
U1	5444(1)	8932(1)	1285(1)	15(1)	6.29
U2	–290(1)	6004(1)	3627(1)	14(1)	6.19
U3	2059(1)	8722(1)	1226(1)	14(1)	6.07
U4	3110(1)	5786(1)	3648(1)	14(1)	6.16
S1	1232(10)	1251(9)	–1263(8)	15(2)	5.83
S2	3706(9)	3844(9)	6341(8)	16(2)	6.30
*M*1	0	1/2	0	22(4)	1.91
*M*2	1/2	0	1/2	16(4)	1.81
*M*3	0	0	1/2	20(5)	2.03
O1	2810(30)	7020(20)	4170(20)	34(7)	1.95
O2	6090(20)	487(18)	–225(17)	16(5)	1.93
O3	4410(20)	4593(18)	6514(17)	12(5)	2.06
O4	4480(20)	60(20)	1933(18)	19(5)	1.90
O5	1150(20)	918(19)	–130(18)	18(5)	2.04
O6	1190(20)	5239(18)	4750(17)	17(5)	1.93
O7	2710(20)	716(17)	–1720(16)	10(5)	1.73
O8	510(20)	4630(20)	3182(19)	25(6)	1.80
O9	410(20)	603(19)	–1485(17)	17(5)	1.89
O10	4240(20)	2424(18)	6860(17)	13(5)	2.06
O11	770(20)	2741(18)	–1712(16)	10(5)	1.79
O12	2270(20)	4300(19)	6718(18)	17(5)	1.98
O13	1730(20)	9697(18)	2030(16)	12(5)	1.80
O14	–1210(20)	7460(20)	3980(20)	28(6)	1.71
O15	3590(20)	4482(19)	3091(18)	20(5)	1.68
O16	3960(20)	4032(19)	5178(19)	20(5)	1.94
O17	1420(20)	7033(19)	2643(17)	17(5)	1.86
OH18	4050(20)	7255(19)	1927(18)	21(5)	1.33
O19	2280(20)	7850(20)	330(19)	26(6)	1.65
O20	6470(20)	7720(20)	700(20)	29(6)	1.80
OW21	4070(20)	8790(20)	4730(20)	32(6)	0.30
OW22	1820(20)	140(20)	3878(19)	29(6)	0.32
OW23	9170(30)	9890(20)	3890(20)	41(7)	0.37
OW24	9360(20)	2110(20)	4390(20)	29(6)	0.33
OW25	1060(20)	3010(20)	750(20)	35(6)	0.32
OW26	6060(30)	430(20)	3380(20)	39(7)	0.31
OW27	–1540(20)	4920(20)	1388(19)	29(6)	0.31
OW28	1130(30)	5700(20)	560(20)	40(7)	0.33
OW29	3400(20)	1730(20)	4500(20)	33(6)	0.30
OW30	2480(30)	2700(30)	2230(20)	62(9)	0.00
OW31	8820(30)	1800(30)	1900(30)	60(9)	0.00
OW32	3330(30)	7170(30)	6720(30)	76(10)	0.00
OW33	5020(40)	2950(30)	1070(30)	94(12)	0.00
OW34	5870(30)	5260(30)	890(30)	76(10)	0.00

Notes: Bond valence parameters are from Brown and Altermatt (1985) and Burns et al. (1997) (U^{+6} in 7-coordination). Site occupancies for *M* sites: *M*1: Mg = 0.62(4), Mn^{2+} = 0.38(4); *M*2: Mg = 0.72(4), Mn^{2+} = 0.28(4); *M*3: Mg = 0.82(4), Mn^{2+} = 0.18(4). All other positions have full occupancy.

TABLE 4. Anisotropic-displacement parameters (Å^2 × 10^3) for the cations in the structure of marecottite

	*U_{11}	U_{22}	U_{33}	U_{12}	U_{13}	U_{23}
U1	8(1)	20(1)	14(1)	3(1)	–4(1)	–8(1)
U2	7(1)	20(1)	12(1)	3(1)	–4(1)	–8(1)
U3	7(1)	19(1)	14(1)	3(1)	–3(1)	–8(1)
U4	6(1)	19(1)	13(1)	3(1)	–3(1)	–7(1)
S1	15(5)	19(5)	6(5)	1(4)	0(4)	–8(4)
S2	11(5)	18(5)	19(6)	–3(4)	–8(4)	–4(4)
*M*1	23(7)	20(7)	18(8)	–8(5)	3(6)	–6(5)
*M*2	18(7)	23(7)	12(8)	–15(6)	4(6)	–5(5)
*M*3	18(8)	20(8)	21(9)	–9(6)	–2(6)	–2(6)

* The anisotropic displacement factor exponent takes the form: $-2\pi^2[h^2a^{*2}U_{11} + ... + 2\,h\,k\,a^*\,b^*\,U_{12}]$

TABLE 5. Selected interatomic distances (Å) and angles (º) in the structure of marecottite

U1-O4a	1.72(2)	S2-O3	1.44(2)
U1-O20	1.75(2)	S2-O10	1.45(2)
U1-O2a	2.22(2)	S2-O12	1.46(2)
U1-O2b	2.30(2)	S2-O16	1.49(2)
U1-O7b	2.45(2)	**<S2-O>**	**1.46**
U1-O10c	2.46(2)		
U1-OH18	2.53(2)	*M*1-OW28, e	2.10(2) ×2
<U1-O_{Ur}>	**1.73**	*M*1-OW25, e	2.12(2) ×2
<U1-ϕ_{eq}>	**2.39**	*M*1-OW27, e	2.12(2) ×2
		<*M*1-ϕ>	**2.11**
U2-O8	1.74(2)		
U2-O14	1.78(2)	*M*2-OW26, f	2.12(3) ×2
U2-O6d	2.24(2)	*M*2-OW21c, g	2.14(2) ×2
U2-O6	2.28(2)	*M*2-OW29, f	2.14(2) ×2
U2-O17	2.30(2)	**<*M*2-ϕ>**	**2.13**
U2-O12d	2.49(2)		
U2-O11e	2.57(2)	*M*3-OW23h, c	2.05(3) ×2
<U2-O_{Ur}>	**1.76**	*M*3-OW24i, f	2.11(2) ×2
<U2-ϕ_{eq}>	**2.38**	*M*3-OW22, j	2.12(2) ×2
		<*M*3-ϕ>	**2.09**
U3-O13	1.75(2)		
U3-O19	1.79(2)	O4a-U1-O20	176.4(11)
U3-O17	2.24(2)	O8-U2-O14	174.3(11)
U3-O2b	2.30(2)	O13-U3-O19	174.6(10)
U3-OH18	2.42(2)	O1-U4-O15	174.6(11)
U3-O9e	2.46(2)		
U3-O5a	2.51(2)	O5-S1-O9	112.5(13)
<U3-O_{Ur}>	**1.77**	O5-S1-O11	106.6(12)
<U3-ϕ_{eq}>	**2.39**	O9-S1-O11	110.7(13)
		O5-S1-O7	106.0(13)
U4-O1	1.70(2)	O9-S1-O7	108.4(11)
U4-O15	1.78(2)	O11-S1-O7	112.5(12)
U4-O6	2.29(2)	**<O-S2-O>**	**109.4**
U4-O17	2.34(2)		
U4-O16	2.41(2)	O3-S2-O10	109.4(13)
U4-OH18	2.44(2)	O3-S2-O12	109.7(12)
U4-O3c	2.52(2)	O10-S2-O12	112.9(13)
<U4-O_{Ur}>	**1.74**	O3-S2-O16	110.4(13)
<U4-ϕ_{eq}>	**2.40**	O10-S2-O16	105.3(12)
		O12-S2-O16	109.0(14)
S1-O5	1.44(2)	**<O-S2-O>**	**109.4**
S1-O9	1.49(2)		
S1-O11	1.49(2)		
S1-O7	1.53(2)		
<S1-O>	**1.49**		

Notes: a = x,y + 1,z; b = –x + 1,–y + 1,–z; c = –x + 1,–y + 1,–z + 1; d = –x,–y + 1,–z + 1; e = –x,–y + 1,–z; f = –x + 1,–y,–z + 1; g = x,y – 1,z; h = x – 1,y – 1,z; I = x – 1,y,z; j = –x,–y,-z + 1. Bold indicates sums.

TABLE 7. Powder XRD data for marecottite

			Marecottite, La Creusaz*				Marecottite, Jáchymov†	
			d_{calc}	I_{calc}	d_{obs}	I_{obs}	d_{obs}	I_{obs}
0	0	1	12.4	<1			12.7	4
0	$\bar{1}$	1	9.47	100	9.46	100	9.57	100
1	0	1	8.63	8	8.63	20	8.53	31
1	0	$\bar{1}$	7.15	<1	7.17	10		
1	1	2	6.47	6	6.46	20		
$\bar{1}$	1	0	6.29	5	6.33	20	6.38	23
0	1	2	6.31	1				
0	2	0	4.980	3	5.00	10		
0	2	2	4.740	24	4.73	80	4.797	56
0	1	3	4.380	2	4.37	5		
2	0	2	4.310	2	4.33	5		
1	1	$\bar{2}$	4.160	2	4.17	10	4.176	29
2	2	0	4.080	3	4.08	10		
2	1	3	3.970	4	3.98	10		
2	$\bar{1}$	1	3.890	3	3.9	10	3.903	20
0	2	3	3.890	1				
1	0	$\bar{3}$	3.590	2	3.58	10	3.561	10
2	0	$\bar{2}$	3.570	2				
0	1	$\bar{3}$	3.440	13	3.44	80	3.438	81
3	1	0	3.420	11				
3	2	1	3.397	10				
0	$\bar{2}$	2	3.380	9	3.39	70	2.361	3
0	3	3	3.160	5	3.16	20	3.201	23
0	0	4	3.110	7	3.11	20	3.123	2
$\bar{3}$	0	1	3.070	8	3.08	20	3.068	43
3	3	$\bar{2}$	3.010	7	3.01	10	3.017	3
0	3	$\bar{1}$	2.970	6	2.98	10	2.928	3
3	0	3	2.876	8	2.88	30	2.852	44
3	1	4	2.772	6	2.78	20	2.787	4
3	$\bar{1}$	2	2.731	4	2.74	20	2.734	29
4	1	1	2.679	1			2.679	7
0	4	2	2.636	1	2.64	10	2.65	1
0	1	5	2.630	3				
$\bar{3}$	1	2	2.588	2	2.59	10	2.586	13
3	4	3	2.530	1	2.53	10	2.558	4
0	4	0	2.490	1	2.491	20	2.4926	3
3	2	5	2.488	3			2.4787	4
3	$\bar{2}$	1	2.429	3	2.433	20	2.4527	12
3	3	$\bar{2}$	2.172	4	2.173	20 b	2.1557	19
many lines…					2.139	20 b	etc…	
					2.108	20 b		
					2.09	20 b		
					2.014	10 b		
					1.947	10 b		
					1.834	5 b		
					1.751	20 b		
					1.713	20 b		
					1.692	20 b		

* Gandolfi camera, 114.6 mm diameter, Cu$K\alpha$ Ni-filtered X-radiation. Intensities were visually estimated. Powder pattern calculated using CrystalDiffract by David Palmer, for the structure model of Table 3. The following lines could not be indexed: 7.58/1; 6.99/1; 6.87/1; 5.992/13; 5.167/7; 4.421/3; 4.274/33; 3.749/11; 3.670/1; 3.640/6; 3.484/11; 3.361/3; 2.709/9.
† Ondrus et al. (1997b).

2.37(9) Å derived from many well-refined structures by Burns et al. (1997). The bond-valence sums incident upon the U^{6+} sites, calculated using the parameters of Burns et al. (1997), range from 6.07 to 6.29, in agreement with the assignment of all U as U^{6+}.

The structure contains three symmetrically distinct *M* sites, each of which is located on a center of symmetry and coordinated by six H_2O groups in an octahedral arrangement. The average *M*-H_2O bond lengths range from 2.09 to 2.13 Å. Following the results of chemical analysis, refinement of the occupancies of these sites using the scattering factors of Mg and Mn gave: *M*1: Mg = 0.62(4), Mn^{2+} = 0.38(4); *M*2: Mg = 0.72(4), Mn^{2+} = 0.28(4); *M*3: Mg = 0.82(4), Mn^{2+} = 0.18(4). The average Mg/Mn ratio deduced from the structure refinement is 2.57, which is in reasonably good agreement with the ratio obtained from the semi-quantitative EMP analyses (3.5).

There are two symmetrically distinct S^{6+} sites in the structure, each of which is tetrahedrally coordinated by four O atoms, with average S-O bond-lengths of 1.49 and 1.46 Å for the S1 and S2 polyhedra, respectively. The bond-valence sums incident at these sites, calculated using the parameters for S^{6+}-O from Brown and Altermatt (1985), are 5.83 and 6.30 *vu* for the S1 and S2 sites, respectively.

Structural formula

With the exception of the three *M* cations that are located on centers of symmetry, all atoms are located on general positions in space group $P\bar{1}$. The anions were readily designated as O, OH^-, and H_2O on the basis of the bond-valence sums incident upon each site (Table 3); there are 19 O, 1 OH, and 14 H_2O sites. The structural formula for the crystal studied is therefore $(Mg_{2.18}Mn_{0.82})(H_2O)_{18}[(UO_2)_4O_3(OH)(SO_4)_2]_2(H_2O)_{10}$, Z = 1, where the constituents contained with the sheets of uranyl and sulfate polyhedra are enclosed by brackets.

Structural connectivity

The four symmetrically distinct uranyl pentagonal bipyramids share equatorial edges, forming chains that are two polyhedra wide (Fig. 3e). Adjacent chains of uranyl polyhedra are linked into sheets (Fig. 3e) by the sharing of equatorial vertices of the uranyl pentagonal bipyramids with sulfate tetrahedra, such that each sulfate tetrahedron is linked to four different uranyl pentagonal bipyramids. The $M(H_2O)_6$ octahedra are located in the interlayer between the uranyl sulfate sheets (Fig. 3f). The perfect cleavage observed along (011) is due to the fact that the $M(H_2O)_6$ octahedrons are connected to the uranyl sulfate sheets on either side by hydrogen bonding only.

Comparison to synthetic zippeite

Vochten et al. (1995) reported the structure of a synthetic zippeite crystal and provided the composition $K(UO_2)_2SO_4(OH)_3\cdot H_2O$. The structure contains sheets of uranyl pentagonal bipyramids and sulfate tetrahedra that are topologically identical to those found in marecottite. However, Vochten et al. (1995) reported that the sheet in zippeite contains more H than what we found in marecottite. They indicated that the sheets contain $Ur O_2(OH)_3$ pentagonal bipyramids, whereas in marecottite, one of the uranyl polyhedra contains only O atoms, and three contain a single OH group. Consideration of the structure reported by Vochten et al. (1995) using the bond-valence parameters proposed by Burns et al. (1997) leads to a rather different interpretation. The anions designated by Vochten et al. (1995) as OH are each bonded to three U^{6+} cations, and the bond-valence sums incident upon the anion sites from the U^{6+}-ϕ bonds are 1.69 and 1.85 v.u., which are inconsistent with either containing OH.

The site with an incident bond-valence of 1.69 may accept an hydrogen bond from an interlayer H_2O group, which would result in a bond-valence sum typical of an O atom. Thus, it appears that the sheets in synthetic K-zippeite do not contain any OH groups, as all of the other anions are either O_{Ur} atoms

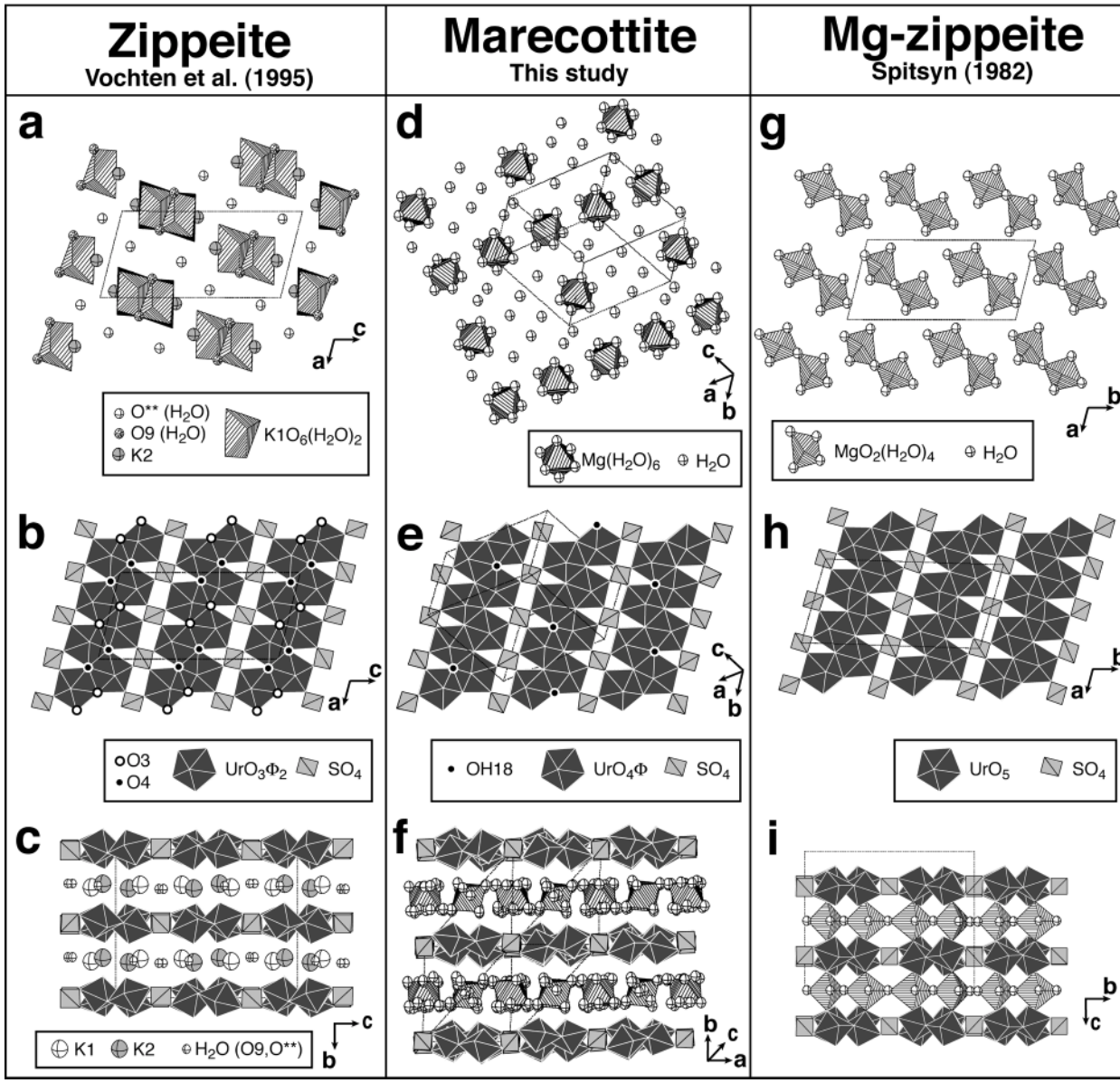

FIGURE 3. Structural relationships between zippeite (Vochten et al. 1995), Mg-zippeite (Spitsyn et al. 1982), and marecottite.

or are shared between uranyl polyhedra and sulfate tetrahedra. There are two O atom positions in the interlayer of the structure, but our bond-valence calculations indicate that each of these correspond to H_2O, rather than one H_2O and one OH as proposed by Vochten et al. (1995). Our bond-valence analysis therefore indicates the formula $K(UO_2)_2(SO_4)O_2 \cdot 2H_2O$, which is problematic because it is not electro-neutral. A re-investigation of the structure of synthetic K-zippeite is therefore in progress.

Comparison to synthetic "Zn-zippeite"

Spitsyn et al. (1982) provided the structure of a synthetic phase that contains zippeite-type uranyl sulfate sheets with Zn cations in the interlayer. In this structure, the Zn cations are octahedrally coordinated by four H_2O groups and two O_{Ur} atoms that belong to the uranyl polyhedra of each adjacent sheet (Fig. 3g, i). This compound has a structure that is significantly different from that of marecottite because the interlayer octahedra are attached to sheets on either side by vertex sharing, whereas in marecottite, the $Mg(H_2O)_6$ octahedra are held in the interlayer by hydrogen bonding only (Fig. 3f,i).

REDEFINITION OF MG-ZIPPEITE

Original description

The original description of Mg-zippeite was made using fine-grained efflorescence from the Lucky Strike no. 2 mine in Emery County, Utah. There, the mineral occurs very sparingly, associated with Na-zippeite, gypsum, bieberite, cobaltocalcite, and rabbittite (Frondel et al. 1976). The mineral description is

TABLE 8. Powder XRD data for Mg-zippeite

Spitzyn et al. (1982) (magnesium-zippeite)*			Lucky Strike no. 2, original magnesium-zippeite†				Lucky Strike no. 2, neotype magnesium-zippeite‡		Magnesium-zippeite, Jáchymov (Ondrus et al. 1997)	
h	*k*	*l*	d_{calc}	I_{calc}	d_{obs}	I_{obs}	d_{obs}	I_{obs}	d_{obs}	I_{obs}
					9.7	10	**9.83**	**20**		
							9.51	**30**		
0	0	$\bar{2}$	8.59	20			8.59	50	8.57	17
0	2	0	7.10	100	7.2	80	7.14	100	7.11	100
0	2	1	6.56	<1			**6.42**	**5**		
1	1	$\bar{2}$	6.21	<1					6.21	5
1	$\bar{1}$	1	6.21	<1						
0	2	2	5.47	14			5.49	10	5.48	17
1	1	$\bar{3}$	5.03	<1	4.9	10				
1	1	2	5.03	<1						
							4.75	**10d**		
0	0	$\bar{4}$	4.30	7			4.27	20	4.29	13
2	0	2	4.20	6	4.2	10	4.21	20	4.19	13
$\bar{2}$	0	0	4.19	6						
1	3	$\bar{1}$	4.12	<1					4.13	4
1	3	0	4.12	2						
1	1	$\bar{4}$	4.09	1					4.08	1
1	$\bar{1}$	3	4.09	<1						
$\bar{1}$	3	2	3.90	7	3.9	10	3.926	20	3.91	15
0	2	4	3.68	4			3.648	10	3.674	9
2	2	2	3.61	4	3.58	100	3.562	40	3.613	10
$\bar{2}$	2	0	3.61	5						
1	3	2	3.55	2					3.559	58
0	$\bar{4}$	0	3.55	23						
2	0	$\bar{4}$	3.45	22	3.48	80	3.453	80	3.449	38
2	0	2	3.45	22						
0	4	2	3.28	4			3.284	10	3.288	11
1	3	$\bar{4}$	3.17	<1					3.181	4
1	3	3	3.17	<1						
2	2	$\bar{4}$	3.10	28	3.11	60	3.116	80	3.104	40
2	2	2	3.10	28						
							3.063	10		
0	0	6	2.86	13	2.88	20	2.858	50	2.859	19
1	$\bar{3}$	4	2.81	1					2.811	4
0	4	4	2.74	2	2.74	30	2.730	20d	2.738	3
$\bar{2}$	4	2	2.71	2					2.714	6
2	$\bar{4}$	0	2.71	2						
$\bar{2}$	0	6	2.69	1					2.691	6
2	0	4	2.69	1						
0	2	$\bar{6}$	2.66	16			2.648	50	2.653	22
1	5	$\bar{2}$	2.62	3					2.632	13
$\bar{2}$	2	6	2.517	1	2.52	20			2.515	6
2	$\bar{2}$	4	2.516	1						
2	4	$\bar{4}$	2.474	9	2.49	10	2.481	40	2.4774	21
2	4	2	2.474	8						
0	$\bar{6}$	0	2.365	3			2.377	5	2.3731	16
0	6	2	2.280	3			2.287	5	2.2873	10
0	4	6	2.229	8			2.230	20	2.2293	12
4	0	2	2.163	8			2.176	10	2.1614	9
2	4	$\bar{6}$	2.144	1					2.1444	4
2	$\bar{4}$	4	2.144	1						
$\bar{2}$	0	8	2.136	2			2.132	10	2.1317	7
2	0	6	2.135	2						
$\bar{4}$	0	4	2.098	2					2.0968	5
4	0	0	2.097	2			2.078	30		
$\bar{4}$	2	2	2.069	7					2.0686	12
0	2	8	2.056	2			2.045	5	2.052	3
2	2	8	2.045	2			2.025	5	2.0432	8
2	2	6	2.044	2			1.959	40		
$\bar{4}$	2	4	2.012	2					2.0116	5
4	2	0	2.0113	2						
1	3	8	2.0062	1					2.0027	1
$\bar{3}$	5	0	1.9919	1					1.9919	1
1	7	$\bar{1}$	1.9705	1					1.9759	5
2	6	$\bar{4}$	1.9512	5			1.949	5	1.9518	22
2	$\bar{6}$	2	1.9510	5						
1	7	2	1.9451	5						
$\bar{4}$	0	6	1.9323	1					1.931	5
4	0	2	1.9317	1						

* Powder pattern calculated using CrystalDiffract by David Palmer, using the structure model for Zn isomorph, the cell dimension of the Mg-end-member, and scattering factors for Mg. The following lines were not indexed: 7.59/5; 7.48/8; 3.75/3; 3.244/2; 3.225/1; 3.041/3; 2.950/5; 2.0278/1; 1.9575/5; 1.99546/7; 1.7144/2.

† Frondel et al. (1976).

‡ Gandolfi camera, 114.6 mm diameter, Cu$K\alpha$ Ni-filtered X-radiation. Intensities were visually estimated.

TABLE 8.—*Continued*

Spitzyn et al. (1982) (magnesium-zippeite)*			Lucky Strike No. 2, original magnesium-zippeite†				Lucky Strike no. 2, neotype magnesium-zippeite‡		Magnesium-zippeite, Jáchymov (Ondrus et al. 1997)	
h	*k*	*l*	d_{calc}	I_{calc}	d_{obs}	I_{obs}	d_{obs}	I_{obs}	d_{obs}	I_{obs}
$\bar{1}$	7	$\underline{3}$	1.8971	2			1.905	5	1.9022	4
4	4	$\underline{2}$	1.8468	6			1.859	10	1.8477	5
0	6	6	1.8237	4			1.828	20	1.8268	8
$\bar{3}$	5	6	1.7878	2			1.784	5	1.7885	4
0	$\underline{8}$	0	1.7738	2			1.743	20	1.7798	12
1	$\underline{7}$	$\underline{4}$	1.7533	3			1.737	10	1.7572	4
2	0	$\underline{\bar{1}0}$	1.7472	3					1.7439	10
$\underline{2}$	0	8	1.7467	2						
$\underline{\bar{4}}$	0	8	1.7265	3					1.7243	9
4	0	4	1.7258	3						
0	0	$\underline{10}$	1.7186	1					1.7163	2
2	$\underline{2}$	$\underline{\bar{1}0}$	1.6965	6			1.694	30	1.6945	13
2	$\underline{\bar{2}}$	8	1.6961	5						

* Powder pattern calculated using CrystalDiffract by David Palmer, using the structure model for Zn isomorph, the cell dimension of the Mg-end-member, and scattering factors for Mg. The following lines were not indexed: 7.59/5; 7.48/8; 3.75/3; 3.244/2; 3.225/1; 3.041/3; 2.950/5; 2.0278/1; 1.9575/5; 1.99546/7; 1.7144/2.
† Frondel et al. (1976).
‡ Gandolfi camera, 114.6 mm diameter, Cu$K\alpha$ Ni-filtered X-radiation. Intensities were visually estimated.

based on a poor powder XRD pattern (Table 8) and a bulk-chemical analysis (Table 1). No indexing of reflections is available for the powder diagram of any natural zippeite containing a divalent cation, as none of the zippeites with divalent cations synthesized by Frondel et al. (1976) were suitable for single-crystal XRD studies. All the reflections observed by Frondel et al. (1976) are present in the powder XRD pattern of marecottite (Table 7), although there is poor agreement among the intensities. The micro-chemical analysis of 12 mg of hand-picked sample showed the Lucky Strike Mg-zippeite to be a basic Mg uranyl sulfate (Table 1), but Frondel et al. (1976) considered the data to be semi-quantitative at best, due to the difficulty in separating pure material from the fine-grained mixture.

Re-evaluation of the type material

A catalog search of Harvard Mineralogical Museum revealed the type specimen for zippeite, but nothing for Mg-zippeite. A search of Frondel's research collection unearthed one specimen from the Mg-zippeite type locality (Lucky Strike no. 2), sampled by Mary Weeks (sample AW87-52). However, there is no evidence that this sample is part of the original type material, or that the type material has been preserved. The specimen consists of fine-grained orange powder in the bottom of a vial. A portion of this material has been used for an SEM and powder XRD study. The qualitative chemical analysis using the EDS system of the SEM reveals that this material consists of U, S, O, Mg, and Co as major components and Zn, Ni, Cu, and Na as minor elements. The major lines in the Powder X-ray pattern (Table 8) are similar to those given by Frondel (1976). The International Mineralogical Association formally accepted AW87-52 as a neotype for Mg-zippeite, and also agreed to redefine Mg-zippeite as discussed below.

Comparison of the powder XRD pattern of the neotype with the patterns of marecottite and of Spitsyn et al. (1982)'s synthetic $Mg(H_2O)_{3.5}(UO_2)_2(SO_4)O_2$ reveal that the neotype is probably a mixture of marecottite and $Mg(H_2O)_{3.5}(UO_2)_2(SO_4)O_2$. We therefore use this analogy to redefine Mg-zippeite as a natural compound identical with synthetic $Mg(H_2O)_{3.5}(UO_2)_2(SO_4)O_2$. Further evidence for the existence of $Mg(H_2O)_{3.5}(UO_2)_2(SO_4)O_2$ in nature is provided by Ondrus et al. (1997a, 1997b), who presented a powder XRD pattern of Mg-zippeite from Jáchymov that closely matches the calculated pattern for $Mg(H_2O)_{3.5}(UO_2)_2(SO_4)O_2$ (Table 8). They also provided diffraction data for a Mg-uranyl-sulfate that they designated "pseudo-Mg-zippeite," which matches the pattern of marecottite (Table 7).

CONCLUDING REMARKS

The new crystal-chemical data presented in this paper provide a basis on which to improve our understanding of the zippeite-group, which plays a central role in the redistribution of uranium during acid drainage of U-bearing mining and industrial wastes. In the absence of crystals suitable for single-crystal XRD work, Mg-zippeite has been redefined by comparison of the powder XRD pattern of natural samples with that of the synthetic compound characterized by Spitsyn et al. (1982) to be monoclinic, *C*2/m, with the structural formula $Mg(H_2O)_{3.5}(UO_2)_2(SO_4)O_2$. Marecottite is a triclinic member of the zippeite-group, with ideal structural formula $Mg_3(H_2O)_{18}[(UO_2)_4O_3(OH)(SO_4)_2]_2(H_2O)_{10}$. Magnesium-zippeite and marecottite coexist in at least three localities: La Creusaz, Jáchymov, and Lucky Strike.

The details of the zippeite-group have been elusive since the description of the first member of the group in 1830. According to the new structural classification of U minerals, the defining element of the zippeite group is the geometry of the uranyl sulfate sheet ("zippeite-type"). This arrangement is found in zippeite that contains monovalent or divalent cations. In zippeites containing divalent cations in the interlayer, different arrangements of the M^{2+} layers result in different unit cells and space groups. This complexity explains why no solid solution between zippeites containing monovalent and divalent cations has yet been reported.

It is possible to distinguish among the different types of zippeites with powder XRD data, in particular once crystal structural information is available independently. Finch et al. (1997) demonstrated the importance of using available structural data to retrieve paragenetic information for alteration products of U-bearing ores and wastes. Another advantage of structural data is that they allow the estimation of thermody-

namic data for these minerals (e.g., Chen et al. 1999). As more data become available for uranyl sulfates, it will become possible to use these minerals to constrain and map the chemistry of the acid drainage around U-bearing sites, and to constrain important fluid parameters such as pH and concentration of some dissolved metals.

ACKNOWLEDGMENTS

Special thanks to Giovanni Ferraris and Joel Grice for handling the complex IMA proposals, to Mark D. Welch for a helpful review, and to Carl Francis for providing access to Frondel's collection. Portions of this research were funded by the Environmental Management Sciences Program of the United States Department of Energy (DE-FG07-97ER14820) and by a grant from the Swiss National Science Foundation to JB (8220-056519).

REFERENCES CITED

Brown, I.D. and Altermatt (1985) Bond-valence parameters obtained from a systematic analysis of the inorganic crystal structure database. Acta Crystallographica, B41, 244–248.

Burns, P.C. (1999) The crystal chemistry of uranium. In P.C. Burns and R. Finch, Eds., Uranium: Mineralogy, geochemistry and the environment, 38, 23–90. Reviews in Mineralogy, Mineralogical Society of America, Washington, D.C.

——— (2001) A new uranyl sulfate chain in the structure of uranopilite. Canadian Mineralogist, 39, 1139–1146.

Burns, P.C., Ewing, R.C., and Hawthorne, F.C. (1997) The crystal chemistry of hexavalent uranium: polyhedron geometries, bond-valence parameters and polymerization of polyhedra. Canadian Mineralogist, 35, 1551–1570.

Cejka, J. (1999) Infrared spectroscopy and thermal analysis of uranyl minerals. In P.C. Burns and R. Finch, Eds., Uranium: Mineralogy, geochemistry and the environment, 38, 521–622. Reviews in Mineralogy, Mineralogical Society of America, Washington, D.C.

Cejka, J., Urbanec, Z., Cejka, J.J., and Mrazek, Z. (1988) Contribution to the thermal analysis and crystal chemistry of johannite $Cu[(UO_2)_2(SO_4)_2(OH)_2].8H_2O$. Neues Jahrbuch für Mineralogie, Abhandlungen, 159, 297–309.

Cejka, J., Sejkora, J., Mrazek, Z., Urbanec, Z., and Járchovsky, T. (1996) Jachymovite, $(UO_2)_8(SO_4)(OH)_{14}\cdot 13H_2O$, a new uranyl mineral from Jàchymov, the Krusné Hory Mts., Czech Republic, and its comparison with uranopilite. Neues Jahrbuch für Mineralogie, Abhandlungen, 170, 155–170.

Chen, F.R., Ewing, R.C., and Clark, S.B. (1999) The Gibbs free energies and enthalpies of formation of U^{6+} phases: An empirical method of prediction. American Mineralogist, 84, 650–664.

Cox, J.D., Wagman, D.D., and Medvedev, V.A. (1989) Codata key values for thermodynamics, 271 p. Hemisphere Publications, New York.

Deliens, M. and Piret, P. (1993) La rabejacite, $Ca(UO_2)_4(SO_4)_2(OH)_6\cdot 6H_2O$, nouveau sulfate d'uranyle et de calcium des gîtes du Lodévois, Hérault, France. European Journal of Mineralogy, 5, 873–877.

Dermot, H. and Brugger, J. (2000) Mineralogy of acid mine drainage at Ranger Mine, Northern Territories, Australia. Abstract for the Fourth International Conference on Minerals and Museum, Melbourne, December 2000.

Edwards, K.J., Bond, P.L., Druschel, G.K., McGuire, M.M., Hamers, R.J., and Banfield, J.F. (2000) Geochemical and biological aspects of sulfide mineral dissolution: lessons from Iron Mountain, California. Chemical Geology, 169, 383–397.

Evangelou, V.P. and Zhang, Y.L. (1995) A review—pyrite oxidation mechanisms and acid mine drainage prevention. Critical Reviews in Environmental Science & Technology, 25, 141–199.

Fernandes, H.M., Veiga, L.H.S., Franklin, M.R., Prado, V.C.S., and Taddei, J.F. (1995) Environmental impact assessment of uranium mining and milling facilities; a study case at the Pocos de Caldas uranium mining and milling site, Brazil. In R.J. Allan and W. Salomons, Eds., Heavy metal aspects of mining pollution and its remediation. 52 p. 161–173. Elsevier, Amsterdam-New York.

Finch, R. and Murakami, T. (1999) Systematics and paragenesis of uranium minerals. In P.C. Burns and R. Finch, Eds., Uranium: Mineralogy, geochemistry and the environment, 38, 91–179. Reviews in Mineralogy, Mineralogical Society of America, Washington, D.C.

Finch, R.J., Hawthorne, F.C., Miller, M.L., and Ewing, R.C. (1997) Distinguishing among schoepite, $(UO_2)_8O_2(OH)_{12}\cdot 12H_2O$, and related minerals by X-Ray powder diffraction. Powder Diffraction, 12, 230–238.

Frondel, C., Ito, J., Honea, R.M., and Weeks, A.M. (1976) Mineralogy of the zippeite-group. Canadian Mineralogist, 14, 429–436.

Gillieron, F. (1988) Zur Geologie der Uranmineralisation in den Schweizer Alpen. Beiträge zur Geologie der Schweiz, Geotechnische Serie, 77, 60 p.

Grenthe, I., Fuger, J., Konings, R.J.M., Lemire, R.J., Muller, A.B., Nguyen-Trung Cregu, C., and Wanner, H. (1992) Chemical thermodynamics of uranium. Elsevier, New York.

Haidinger, W. (1845) Handbuch der bestimmenden Mineralogie, Vienna.

Ibers, J.A. and Hamilton, W.C. (1974) International Tables for X-Ray Crystallography, Vol. IV. The Kynoch Press, Birmingham, U.K.

Meisser, N. and Ansermet, S. (1996) Mineralogy and ^{230}Th-^{234}U dating of an exceptional secondary uranium mineral association of the Aiguilles Rouges massif, Switzerland. Acta Mineralogica-Petrographica, Szeged, XXXVII, Supplementum, M&M3 Conference, Budapest, p. 75.

Meisser, N. and Beck, B. (2000) La genèse des séléniures de bismuth et de plomb de la minéralisation d'uranium de La Creusaz, Massif des Aiguilles Rouges (Valais, Suisse): apport des isotopes du plomb. Abstract for Metallogeny 2000, review and perspectives, December 2000, Nancy, France, 101–102.

Meisser, N., Brugger, J., and Lahaye, Y. (2002) Mineralogy and acid-mine drainage of La Creusaz uranium prospect, Switzerland, 147–150. International Workshop "Uranium Deposits: from their Genesis to their Environmental Aspects", B. Kribek and J. Zeman, Eds., Czech Geological Survey, Prague, ISBN 80-7075-583-0.

Mereiter, K. (1982) Die Kristallstruktur des Johannites, $Cu(UO_2)_2(OH)_2(SO_4)_2\cdot 8H_2O$. Tschermaks Mineralogischen und Petrographischen Mitteillungen, 30, 47–57.

——— (1986) Crystal structure and crystallographic properties of a schröckingerite from Joachims-thal. Tschermaks Mineralogischen und Petrographischen Mitteillungen, 35, 1–18.

Ondrus, P., Veselovsky, F., Hlousek, J., Skála, R., Vavrín, I., Fryda, J., Cejka, J., and Gabasová, A. (1997a) Secondary minerals of the Jáchymov (Joachimsthal) ore district. Journal of the Czech Geological Society, 42, 3–76.

Ondrus, P., Veselovsky, F., Skála, R., Císarová, I., Hlousek, J., Fryda, J., Vavrín, I., Cejka, J., and Gabasová, A. (1997b) New naturally occurring phases of secondary origin from Jáchymov (Joachimsthal). Journal of the Czech Geological Society, 42, 77–107.

Pfeifer, H., Vust, M., Meisser, N., Doppenberg, R., Torti, R., Domergue, F., Keller, C., and Hunziker, J. (1994) Uranium-enrichment in soils and plants in the vicinity of a pitchblende vein at La Creusaz, Les Marérottes (W of Martigny, Valais, Switzerland). Eclogae Geologicae Helveticae, 87, 491–501.

Sejkora, J., Cejka, J., and Ondrus, P. (2000) New data of rabejacite (Jachymov, the Krusne hory Mts., Czech Republic). Neues Jahrbuch für Mineralogie Monatshefte, 289–301.

Shock, E.L., Sassani, D.C., and Betz, H. (1997) Uranium in geologic fluids - estimates of standard partial molal properties, oxidation potentials, and hydrolysis constants at high temperatures and pressures. Geochimica et Cosmochimica Acta, 61, 4245–4266.

Spitsyn, V., Kovba, L., Tabachenko, V., Tabachenko, N., and Mikhaylov, Y. (1982) To the investigation of basic uranyl salts and polyuranates. Izv Akd Nauk SSSR, Ser Kim, 1982, 807–812 (in Russian).

Stüssi-Lauterburg, J. (1995) Historischer Abriss zur Frage einer Schweizer Nuklearbewaffnung. 49 pp. Eidgenössischen Militärbibliothek, Bern.

Thury, M. and Bossart, P. (1999) The Mont Terri rock laboratory, a new international research project in a Mesozoic shale formation, in Switzerland. Engineering Geology, 52, 347–359.

Vinard, P., Blumling, P., McCord, J.P., and Aristorenas, G. (1993) Evaluation of hydraulic underpressures at Wellenberg, Switzerland. International Journal of Rock Mechanics & Mining Sciences & Geomechanics Abstracts, 30, 1143–1150.

Vochten, R., Van Haverbeke, L., and Van Springel, K. (1995) The structural and physicochemical characteristics of synthetic zippeite. Canadian Mineralogist, 33, 1091–1101.

Vochten, R., Blaton, N., and Peeters, O. (1997) Deliensite, $Fe(UO_2)_2(SO_4)_2(OH)_2\cdot 3H_2O$, a new ferrous uranyl sulfate hydroxyl hydrate from Mas d'Alavry, Lodève, Hérault, France. European Journal of Mineralogy, 35, 1021–1025.

MANUSCRIPT RECEIVED FEBRUARY 19, 2002
MANUSCRIPT ACCEPTED DECEMBER 11, 2002
MANUSCRIPT HANDLED BY MARK WELCH